

Study of design parameters on flutter stability of cable-stayed-suspension hybrid bridges

Xin-jun Zhang[†]

Department of Civil Engineering, Zhejiang University of Technology, Hangzhou 310032, China
(Received June 24, 2005, Accepted June 20, 2006)

Abstract. The cable-stayed-suspension hybrid bridge is a cooperative system developed from the traditional cable-stayed and suspension bridges, and takes some advantages of the two bridge systems. It is also becoming a competitive design alternative for some long and super long-span bridges. But due to its great flexibility, the flutter stability plays an important role in the design and construction of this bridge system. Considering the geometric nonlinearity of bridge structures and the effects of nonlinear wind-structure interaction, method and its solution procedure of three-dimensional nonlinear flutter stability analysis are firstly presented. Parametric analyses on the flutter stability of a cable-stayed-suspension hybrid bridge with main span of 1400 meters are then conducted by nonlinear flutter stability analysis, some design parameters that significantly influence the flutter stability are pointed out, and the favorable structural system of the bridge is also discussed based on the wind stability.

Keywords: cable-stayed-suspension hybrid bridges; flutter stability; design parameters.

1. Introduction

The cable-stayed-suspension hybrid bridge is developed from the traditional cable-stayed bridge and suspension bridge, and has some following advantages: (1) As compared to the suspension bridge with the same span length, the suspension portion is greatly shortened, so the tensional forces in the main cables are greatly decreased, which helps to decrease the construction costs of the main cables and the massive anchors, and the difficulty of constructing them in water, and therefore makes it possible to build in the soft soil foundation. In addition, different structural materials can be used in the suspension and cable-stayed portions. For example, the prestressed concrete girder in the cable-stayed portion and the light steel box girder in the suspension portion, and the materials in the deck can be also saved. (2) As compared to the cable-stayed bridges with the same span length, the cable-stayed portion is also greatly shortened, the height of towers and the axial compressive forces in the deck are consequently reduced. In addition, the cantilevers during erection are also greatly shortened, and the wind stability of the bridge under construction is therefore improved.

As a result, it can make up the deficiencies in the structural behavior, construction, economy and the wind stability of the traditional suspension bridge and cable-stayed bridge, and becomes an attractive alternative in the design of long and super long-span bridges.

[†] Associate Professor, Postdoctor, Corresponding Author, E-mail: xjzhang@zjut.edu.cn

The idea of using cables and stay cables to support bridge spans was conceived by Roebling (Balsamo and Drewery 1989), Dischinger (Narasimha 1991), Steinmann (Finzi and Castllani 1992) and Gimsing (1992,1997) etc., but few cable-stayed-suspension hybrid bridges were built before 1920s. After that, this bridge system was used in the rehabilitations of some existing suspension bridges such as the Brooklyn Bridge in America, the Tancarville Bridge in France, the Salazar Bridge in Portugal, etc., and also was proposed in the design of many strait-crossing bridges such as the Great Belt East Bridge (Gimsing 1992), the Gibraltar Bridge (Ostenfeld 1992, Lin and Chow 1991), the Messina Strait Bridge (Finzi and Castllani 1992, Bulson, *et al.* 1983), the Izmit bridge in Turkey (Gimsing 1997), the Tagus River Bridge in Portugal, the Bali Strait Bridge in Java, the and some strait bridges in Japan (Hu 2000). Due to the limitation of computational technique and lack of corresponding analytical theory, this bridge system was not realized until 1997. In 1997, the first modern cable-stayed-suspension hybrid bridge in the world was built in China with a main span of 288 meters (Meng, *et al.* 1999). In the 21st century, many long and particularly super long-span bridges were planned in sea-crossing engineering projects. Many of them were built under the natural conditions unfavorable for building cable-stayed bridge or suspension bridge, such as soft soil foundation, violent typhoon, and the deep-water foundation etc. However, due to its advantages mentioned above, the cable-stayed-suspension hybrid bridge becomes a competitive alternative for designing of these bridges.

The design of cable-stayed-suspension hybrid bridges involves problems of the static and dynamic behavior, construction, economy, and wind stability etc., which need to be fully investigated. In previous studies, more attentions were paid to the static and dynamic behaviors under dead and service loads, the economics, etc. (Meng, *et al.* 1999, Xiao 1999, 2000, Zen, *et al.* 2002, Hu 2000), but few investigations were done on the flutter stability of cable-stayed-suspension hybrid bridges (Sato, *et al.* 2000, Fumoto, *et al.* 2004). Just like the suspension and cable-stayed bridges, the cable-stayed-suspension hybrid bridge is also a structural system of great flexibility, and very susceptible to wind action. The wind stability also becomes a governing factor for the design of this bridge system, and should be fully investigated.

In this paper, based on the method of three-dimensional nonlinear flutter stability analysis, in which the geometric nonlinearity of bridge structures and the effects of nonlinear wind-structure interaction are considered, parametric analyses on the flutter stability of a cable-stayed-suspension hybrid bridge with main span of 1400 meters were conducted, some design parameters that significantly influence the flutter stability are pointed out, and the favorable structural system of the bridge is also discussed based on the wind stability.

2. Method and solution procedure

For long-span cable-supported bridges, the geometric nonlinearity is strong due to the large deformation, cable sag and beam-column effects under the wind loading. In addition, the aerostatic and aerodynamic forces, which are two important types of the wind forces acting on the bridges, are both displacement-dependent and the wind-structure interaction is nonlinear. Therefore, aerodynamic analysis should be conducted on the deformed bridge structures under the static wind action. In general, aerodynamic stability analysis is to obtain the critical condition of aerodynamic stability by gradually increasing the wind speed. In order to consider the effect of nonlinear wind-structure interaction, at every wind speed increment, the nonlinear aerostatic analysis is firstly conducted to predicate the deformed bridge structures under the current wind speed, then on the deformed bridge

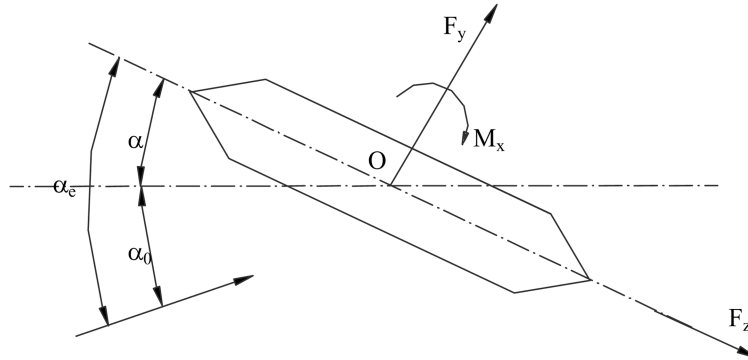


Fig. 1 Aerostatic forces acting on the deck

structures, the aerodynamic response analysis is performed to predicate the response status under the dynamic wind action.

2.1. Nonlinear aerostatic analysis

The aerostatic effect is usually treated as the action of 3 aerostatic components of wind force on the bridge, namely the drag force F_z , lift force F_y and pitch moment M_x as shown in Fig. 1. Assuming that under the effect of the mean wind velocity U with the angle of incidence α_0 , the torsional displacement of deck is α . Then the effective wind angle of attack is $\alpha_e = \alpha_0 + \alpha$. The components of aerostatic forces per unit span acting on the deformed deck can be written as

$$\text{Drag force: } F_z = \frac{1}{2} \cdot \rho U^2 \cdot D \cdot C_z(\alpha_e) \tag{1a}$$

$$\text{Lift force: } F_y = \frac{1}{2} \cdot \rho U^2 \cdot B \cdot C_y(\alpha_e) \tag{1b}$$

$$\text{Pitch moment: } M_x = \frac{1}{2} \cdot \rho U^2 \cdot B^2 \cdot C_M(\alpha_e) \tag{1c}$$

where ρ is the air density; D is the vertical projected area; B is the bridge deck width; $C_z(\alpha_e)$, $C_y(\alpha_e)$, $C_M(\alpha_e)$ are the experimentally measured coefficients of drag force, lift force, and pitch moment respectively.

The aerostatic forces in Eqs. (1a)-(1c) are the function of the torsional displacement of structure. The torsional displacement varies as the girder displaces, and therefore the three components of aerostatic loads are distributed un-uniformly along the bridge deck. For the cables and towers' members, only the drag component is considered.

At a given wind speed U , the static equilibrium equation of structural system under the static wind action can be expressed as

$$[\mathbf{K}(\mathbf{u})]\{\mathbf{u}\} = \mathbf{P}(F_y(\alpha_e), F_z(\alpha_e), M(\alpha_e)) \tag{2}$$

where $[\mathbf{K}(\mathbf{u})]$ is the tangent stiffness matrix which is the sum of elastic stiffness matrix and

geometric stiffness matrix; $\{u\}$ is the nodal displacement vector; $\mathbf{P}(F_y(\alpha_e), F_z(\alpha_e), \mathbf{M}(\alpha_e))$ is the static wind load vector.

Due to the non-linearities of both the bridge structure and the aerostatic forces, Eq. (2) can be solved by the iteration method. The Euclidean Norm of the aerostatic coefficients of lift, drag and pitch moment is taken as convergence criterion, and expressed as (Boonyapinyo, *et al.* 1994)

$$\left\{ \frac{\sum_1^{N_a} [C_K(\alpha_j) - C_K(\alpha_{j-1})]^2}{\sum_1^{N_a} [C_K(\alpha_{j-1})]^2} \right\}^{\frac{1}{2}} \leq \varepsilon_K \quad (K \text{ represents } L, D, M) \quad (3)$$

where ε_K is the prescribed convergence accuracy; N_a is the total number of the nodes subjected to the wind force.

2.2. Nonlinear aerodynamic analysis

The aerodynamic forces acting on the deck usually include the self-excited force due to wind-structure interaction in the smooth oncoming wind flow and the buffeting force due to turbulence in the oncoming wind flow. The buffeting force may not make the bridge aerodynamic unstable, so it is usually neglected in the aerodynamic analysis. The well-known self-excited aerodynamic force i.e., the self-excited lift, L_h , and drag, D_p , as well as the moment, M_α is generally represented as (Scanlan and Jones 1990)

$$\begin{aligned} L_h &= \frac{1}{2}\rho U^2 (2B) \left[KH_1^* \frac{\dot{h}}{U} + KH_2^* \frac{B\dot{\alpha}}{U} + K^2 H_3^* \alpha + K^2 H_4^* \frac{h}{B} + KH_5^* \frac{\dot{p}}{U} + K^2 H_6^* \frac{p}{B} \right] \\ D_p &= \frac{1}{2}\rho U^2 (2B) \left[KP_1^* \frac{\dot{p}}{U} + KP_2^* \frac{B\dot{\alpha}}{U} + K^2 P_3^* \alpha + K^2 P_4^* \frac{p}{B} + KP_5^* \frac{\dot{h}}{U} + K^2 P_6^* \frac{h}{B} \right] \\ M_\alpha &= \frac{1}{2}\rho U^2 (2B^2) \left[KA_1^* \frac{\dot{h}}{U} + KA_2^* \frac{B\dot{\alpha}}{U} + K^2 A_3^* \alpha + K^2 A_4^* \frac{h}{B} + KA_5^* \frac{\dot{p}}{U} + K^2 A_6^* \frac{p}{B} \right] \end{aligned} \quad (4)$$

where H_i^* , A_i^* , P_i^* ($i=1\sim 6$) are the experimentally measured flutter derivatives for the deck under investigation, which are the functions of the reduced frequency $K(=B\omega/U)$ and the effective attack angle α_e due to the static wind action, ω is the response circular frequency.

Eq. (4) represents the aerodynamic force acting on per unit length of the bridge deck. To convert these uniformly distributed force into member end effects, a simple lumping procedure is adopted whereby one-half of the force is assumed to act at each member end. For each element, the equivalent aerodynamic joint load, $\{F\}_i$, is subdivided into stiffness component and damping component as

$$\{F\}_i = \frac{1}{2}\rho U^2 \left([A_s(k, \alpha_e)]_i \{u(x, t)\}_i + \frac{1}{U} [A_d(k, \alpha_e)]_i \{\dot{u}(x, t)\}_i \right) \quad (5)$$

where $\{u(x, t)\}_i, \{\dot{u}(x, t)\}_i$ are the element's displacement and velocity vectors of the aerodynamic response respectively; $[A_s(k, \alpha_e)]_i, [A_d(k, \alpha_e)]_i$ are the element's aerodynamic stiffness and aerodynamic damping matrices respectively represented as follows (Zhang and Sun 2003).

$$\begin{aligned}
 [A_s]_i &= LK^2 \begin{bmatrix} 0 & 0 & 0 & 0 & 0 & 0 & 0 & 0 & 0 & 0 & 0 \\ 0 & H_4^* & H_6^* & -BH_3^* & 0 & 0 & 0 & 0 & 0 & 0 & 0 \\ 0 & P_6^* & P_4^* & -BP_3^* & 0 & 0 & 0 & 0 & 0 & 0 & 0 \\ 0 & -BA_4^* & -BA_6^* & B^2A_3^* & 0 & 0 & 0 & 0 & 0 & 0 & 0 \\ 0 & 0 & 0 & 0 & 0 & 0 & 0 & 0 & 0 & 0 & 0 \\ 0 & 0 & 0 & 0 & 0 & 0 & 0 & 0 & 0 & 0 & 0 \\ 0 & 0 & 0 & 0 & 0 & 0 & 0 & 0 & 0 & 0 & 0 \\ 0 & 0 & 0 & 0 & 0 & 0 & 0 & H_4^* & H_6^* & -BH_3^* & 0 \\ 0 & 0 & 0 & 0 & 0 & 0 & 0 & P_6^* & P_4^* & -BP_3^* & 0 \\ 0 & 0 & 0 & 0 & 0 & 0 & 0 & -BA_4^* & -BA_6^* & B^2A_3^* & 0 \\ 0 & 0 & 0 & 0 & 0 & 0 & 0 & 0 & 0 & 0 & 0 \\ 0 & 0 & 0 & 0 & 0 & 0 & 0 & 0 & 0 & 0 & 0 \end{bmatrix} \\
 [A_d]_i &= BLK \begin{bmatrix} 0 & 0 & 0 & 0 & 0 & 0 & 0 & 0 & 0 & 0 & 0 \\ 0 & H_1^* & H_5^* & -BH_2^* & 0 & 0 & 0 & 0 & 0 & 0 & 0 \\ 0 & P_5^* & P_1^* & -BP_2^* & 0 & 0 & 0 & 0 & 0 & 0 & 0 \\ 0 & -BA_1^* & -BA_5^* & B^2A_2^* & 0 & 0 & 0 & 0 & 0 & 0 & 0 \\ 0 & 0 & 0 & 0 & 0 & 0 & 0 & 0 & 0 & 0 & 0 \\ 0 & 0 & 0 & 0 & 0 & 0 & 0 & 0 & 0 & 0 & 0 \\ 0 & 0 & 0 & 0 & 0 & 0 & 0 & 0 & 0 & 0 & 0 \\ 0 & 0 & 0 & 0 & 0 & 0 & 0 & H_1^* & H_5^* & -BH_2^* & 0 \\ 0 & 0 & 0 & 0 & 0 & 0 & 0 & P_5^* & P_1^* & -BP_2^* & 0 \\ 0 & 0 & 0 & 0 & 0 & 0 & 0 & -BA_1^* & -BA_5^* & B^2A_2^* & 0 \\ 0 & 0 & 0 & 0 & 0 & 0 & 0 & 0 & 0 & 0 & 0 \\ 0 & 0 & 0 & 0 & 0 & 0 & 0 & 0 & 0 & 0 & 0 \end{bmatrix} \tag{6}
 \end{aligned}$$

where L is the element's length.

It is known that the effect of deformation due to the static wind action on the self-excited aerodynamic force is considered in Eq. (5).

On the deformed equilibrium position under the static wind action, the equation of motion under the self-excited aerodynamic loading can be expressed as

$$[M]\{\ddot{u}(x, t)\} + [D]\{\dot{u}(x, t)\} + [K]\{u(x, t)\} =$$

$$\frac{1}{2}\rho U^2 \left([A_s(\mathbf{k}, \alpha_e)] \{ \mathbf{u}(\mathbf{x}, t) \} + \frac{1}{U} [A_d(\mathbf{k}, \alpha_e)] \{ \dot{\mathbf{u}}(\mathbf{x}, t) \} \right) \quad (7)$$

where $[M]$, $[D]$, $[K]$ are the structural mass, damping and tangent stiffness matrices respectively; $\mathbf{u}(\mathbf{x}, t)$, $\dot{\mathbf{u}}(\mathbf{x}, t)$, $\ddot{\mathbf{u}}(\mathbf{x}, t)$ are the structural displacement, velocity and acceleration vectors of the aerodynamic response respectively; $[A_s(\mathbf{k}, \alpha_e)]$, $[A_d(\mathbf{k}, \alpha_e)]$ are the structural aerodynamic stiffness and aerodynamic damping matrices.

To solve Eq. (7), the modal analysis method is used herein, and the aerodynamic response is separated into the spatial (natural mode) and time-dependent (generalized coordinate) components as

$$\{ u(x, t) \} = [\phi(x)] \{ \xi(t) \} \quad (8)$$

where $[\phi(x)]$ is mode matrix obtained from the dynamic characteristics analysis on the deformed bridge structure under the static wind action; $\{ \xi(t) \}$ is the generalized coordinate vector, which can be assumed as a damped harmonic form and represented in the complex plane as

$$\{ \xi(t) \} = \{ \mathbf{R} \} \exp(\lambda t) \quad (9)$$

where $\{ \mathbf{R} \}$ is the response amplitude vector, whose components reflect the participation of each mode in flutter; $\lambda = (\delta + i)\omega$; δ is the response logarithmic decrement; ω is the response angular frequency; $i = \sqrt{-1}$.

Substituting Eqs. (8) and (9) into Eq. (7), then pre-multiplying the transpose of the mode matrix $[\phi(x)]$, and considering the orthogonality between modes and existence of a nontrivial solution, a determinant can be yielded as

$$\left| [M^g] \left(\frac{U}{B} \right)^2 S^2 + [D^g] \left(\frac{U}{B} \right) S + [K^g] - \frac{1}{2} \rho U^2 \left[[A_s^g] + \frac{1}{B} [A_d^g] i K \right] \right| = 0 \quad (10)$$

where, $[M^g] = [\phi(x)]^T [M] [\phi(x)]$, $[D^g] = [\phi(x)]^T [D] [\phi(x)]$, $[K^g] = [\phi(x)]^T [K] [\phi(x)]$ are the generalized mass, damping and stiffness matrices respectively; $[A_s^g] = [\phi(x)]^T [A_s(k, \alpha_e)] [\phi(x)]$, $[A_d^g] = [\phi(x)]^T [A_d(k, \alpha_e)] [\phi(x)]$ are the generalized aerodynamic stiffness and damping matrices; $S = k(\delta + i)$.

Eq. (10) can be solved by the PK-F method (Namini 1992). The value S , which makes the determinant equal to zero, represents the actual response. The logarithmic decrement and the angular frequency of response can be computed as

$$\delta = \frac{\text{Re}(S)}{\text{Im}(S)}, \quad \omega = \frac{U}{B} \text{Im}(S) \quad (11)$$

where Re and Im are the real and imaginary parts of a complex variable respectively.

Depending on the sign of the logarithmic decrement, the response can be defined to be: $\delta < 0$, stable; $\delta = 0$, neutrally stable; $\delta > 0$, unstable. The wind speed that produces the neutrally stable is termed as flutter speed U_f , with the corresponding flutter frequency ω_f .

2.3. Solution procedure

Based on the above method, a computer program of nonlinear flutter stability analysis BSNFA is developed to predicate the flutter stability limits of long-span bridges, the computing flow can be described as follows:

1. Input the geometric and physical data of the bridge, the aerostatic coefficients and flutter derivatives etc.
2. Determine the equilibrium position under the dead load by three-dimensional geometric nonlinear analysis.
3. On the calculated static equilibrium position, loop with the wind speed to find out the flutter wind speed by nonlinear flutter analysis. At each increment of wind speed, the following analysis is performed:
 - (1) Compute the current wind speed U_{cur} , starting with U_{low} and incrementing with U_{inc} , where U_{low} is the initial wind speed.
 - (2) Predicate the aerostatic equilibrium position under current wind speed by three-dimensional nonlinear aerostatic analysis, and the computational flow is described as follows
 - ① Calculate the aerostatic load $\{F_0\}$ under the initial wind attack angles for the previous aerostatic equilibrium state, and let $\{F_2\} = \{F_0\}, \{F_1\} = \{0\}$;
 - ② Calculate the aerostatic load increment $\{\Delta F\} = \{F_2\} - \{F_1\}$, and let $\{F_1\} = \{F_2\}$;
 - ③ Perform structural geometric nonlinear analysis under the incremental aerostatic load, the deformed position is then obtained;
 - ④ Determine the effective wind attack angle of the deck, and calculate the changed aerostatic load $\{F_2\}$;
 - ⑤ Check if the Euclidean norm of aerostatic coefficients is less than the prescribed tolerance. If satisfied, the iteration is convergent. Otherwise repeat steps ② - ④ until Eq. (3) is satisfied or the maximum number of iterations is reached.
 - (3) On the deformed aerostatic equilibrium position, structural dynamic characteristics is analyzed by the subspace iteration method, and the modes are selected to participate in aerodynamic response analysis.
 - (4) Calculate the effective wind attack angle according to the deformation obtained in step (2), the aerodynamic stiffness matrix and the aerodynamic damping matrix are recalculated to take into account the nonlinear and three-dimensional effects of the aerodynamic force. Using the changed dynamic characteristics obtained in step (3), the determinant is established and solved to determine the response state.
 - (5) Check if the aerodynamic response is divergent. If not, the flutter critical condition is not reached, then repeat steps (1)-(4) until the flutter critical condition is reached.
 - (6) Compute the flutter wind speed and the corresponding flutter frequency.

3. Description of the example bridge

The example cable-stayed-suspension hybrid bridge consists of a main span of 1400 m and two side spans of 319 m as shown in Fig. 2, which was proposed for construction in the east channel of Lingding Strait in China (Xiao 2000). The central span consists of the cable-stayed portion of 788 m and the suspension portion of 612 m. The spacing of two main cables is 34 m, the cable sag to span ratio is 1/7.6, and the spacing of hangers is 18 m. The stay cables are anchored to the girder at 18 m intervals in the central span and 14 m in the side spans. The deck is a steel streamlined box steel girder of 36.8 m wide and 3.8 m high. The towers are the door-shaped frames with 3 transverse beams. The sectional and material properties of the bridge are given in Table 1.

The bridge is idealized to a three-dimensional finite element model for flutter stability analysis, in which the girder and towers were modeled by three-dimensional beam elements, the hangers, main

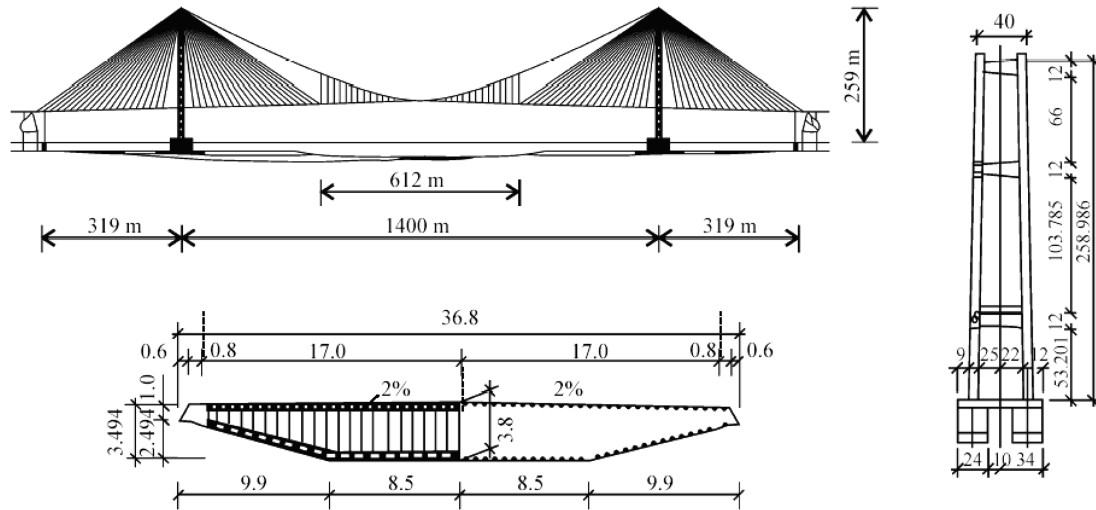


Fig. 2 General configuration of the cable-stayed-suspension hybrid bridge (unit: m)

Table 1 The sectional and material properties of the bridge

Members		E (Mpa)	A (m^2)	J_d (m^4)	I_z (m^4)	I_y (m^4)	M (Kg/m)	J_m (Kg·m ² /m)
Girder		2.1×10^5	1.2481	5.034	1.9842	137.754	18387	1.852×10^6
Main Cable	CS	2.0×10^5	0.3167	0.0	0.0	0.0	2660	0.0
	SS	2.0×10^5	0.3547	0.0	0.0	0.0	2980	0.0
Hanger		2.0×10^5	0.0064	0.0	0.0	0.0	50.2	0.0
Stay cable		2.0×10^5	0.008	0.0	0.0	0.0	62.8	0.0
Towers	C	3.3×10^4	30.0	350.0	320.0	220.0	78000	5.7×10^5
	TB	3.3×10^4	10.0	150.0	70.0	70.0	26000	4.7×10^5

Notes: E -elastic modulus, A -sectional area, J_d -torsional moment of inertia, I_z -vertical bending moment of inertia, I_y -lateral bending moment of inertia, m -mass per unit length, J_m - mass moment of inertia per unit length, CS-center span, SS-side span, C-tower's Column, TB-tower's transverse beam.

cables and stay cables were modeled by three-dimensional bar elements. The connections between bridge components and the supports of the bridge were properly modeled. Since the girder of the bridge was very similar to that of the Runyang Bridge constructed in Jiangshu Province of China, the aerostatic and aerodynamic coefficients of the Runyang Bridge were used in the flutter stability analysis of the bridge (Chen and Song 2000). The damping ratio was taken as 0.5%. It is to be noted that the following flutter stability analyses were all under the wind attack angle of 0°.

4. Parametric analysis

Investigations by Xiao (1999, 2000) and Meng (1999) showed that the static and dynamic characteristics of the cable-stayed-suspension hybrid bridges are greatly influenced by some design parameters such as the cable sag, the suspension length, the arrangement of the stay cable planes,

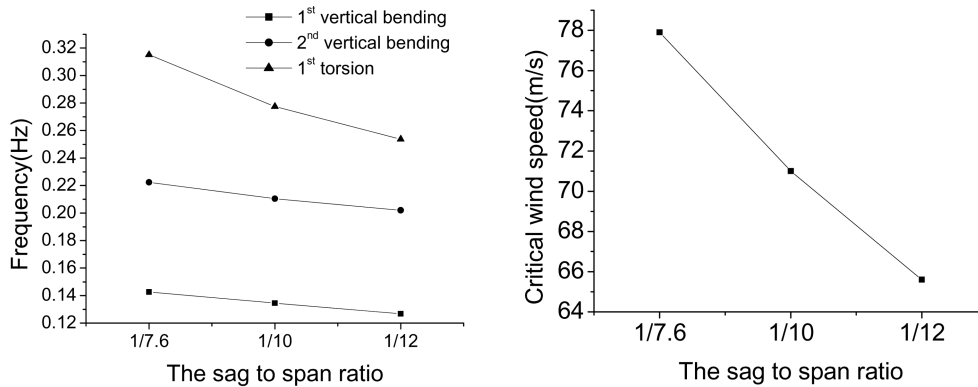


Fig. 3 Evolutions of modal frequencies and the critical wind speed with the sag to span ratio

the subsidiary piers in side spans, and the deck form etc. In the following sections, how these design parameters affect the flutter stability of cable-stayed-suspension hybrid bridges is investigated analytically by the computer program BSNFA.

4.1. Cable sag

The cable sag, being an important design parameter for cable-stayed-suspension hybrid bridges, directly influences the tower's height and the inclination angles of the stay cables, which are closely related to the tensile forces in main cables and stay cables, and ultimately affects structural stiffness and dynamic characteristics of the bridge.

Fig. 3 shows the evolutions of structural frequencies of main modes participating in flutter analysis and the critical wind speed with the sag to span ratio.

The critical wind speed decreases significantly with the decrease of cable sag. It is because that with the reduction of cable sag, the tower's height and the inclination angles of stay cables are both decreased, and the supporting efficiency of the stay cables and further structural stiffness of the bridge are consequently reduced, which leads to the reduction of modal frequencies, particularly the torsional frequencies. Viewed from the aspect of flutter stability, the cable sag should not be too small for the bridge.

4.2. Suspension length

Increasing or shortening the suspension length enables the cable-stayed-suspension hybrid bridge to behave as suspension bridge or cable-stayed bridge. Fig. 4 shows the evolutions of structural frequencies of main modes participating in flutter analysis and the critical wind speed with the suspension to span ratio.

As shown in Fig. 4, the critical wind speed decreases greatly as the suspension length increases. It is because that with increase of suspension length, the bridge behaves gradually as a suspension bridge, structural stiffness and frequencies of the bridge are all reduced. Therefore, it can be concluded that shorter suspension is aerodynamically favorable for the bridge, but the favorable suspension length should be further investigated by considering other factors such as the static behavior and economics etc.

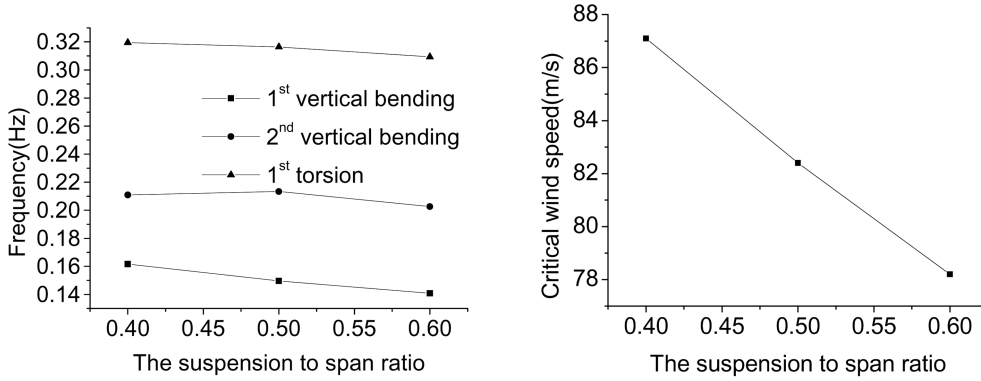


Fig. 4 Evolutions of modal frequencies and the critical wind speed with the suspension to span ratio

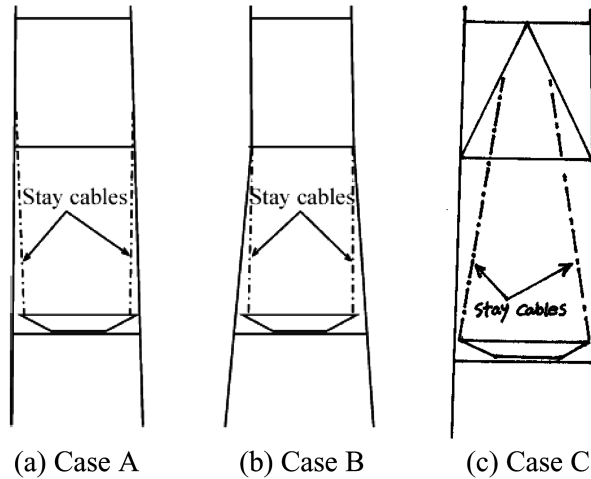


Fig. 5 Different arrangements of the stay cable planes

4.3. Arrangement of the stay cable planes

Likewise, the stay cables of cable-stayed-suspension hybrid bridges can be arranged to be vertical or inclined as cable-stayed bridges, which mainly depends on the lateral configuration of the towers. For the example bridge, the cable planes are inclined inward (Case A) as shown in Fig. 5(a). To investigate the effect of the arrangement of stay cable planes on the flutter stability, two cases are assumed: one is that the cable planes are vertical (Case B) as plotted in Fig. 5(b), and another is that the cable planes are inclined outward (Case C) as shown in Fig. 5(c). Except for the arrangement of cable planes, the other design parameters remain the same for all three cases. The vertical cable planes are achieved by making the anchorage sections of the tower's columns vertical. In order to get the inclined outward cable planes, an inverse V-shaped construction is installed in the position between the upper and middle transverse beams. Table 2 gives the calculated critical wind speeds and structural frequencies under three cases.

As compared to Case A, the critical wind speed is increased by 12 m/s for Case C, and 4.5 m/s

Table 4 Effect of the number of subsidiary piers on the critical wind speed and structural frequencies

Number	0	1	2
Critical wind speed (m/s)	77.9	82.9	84.1
1 st vertical bending (Hz)	0.1360	0.1441	0.1446
2 nd vertical bending (Hz)	0.2032	0.2298	0.2330
1 st torsion (Hz)	0.3051	0.3167	0.3229

Table 5 Effect of the location of subsidiary pier on the critical wind speed and structural frequencies

Locations	1/4 L_s	1/3 L_s	1/2 L_s
Critical wind speed (m/s)	82.9	83.1	83.5
1 st vertical bending (Hz)	0.1442	0.1439	0.1433
2 nd vertical bending (Hz)	0.2303	0.2296	0.2289
1 st torsion (Hz)	0.3164	0.3167	0.3169

Note: L_s is the length of side span.

4.5. Subsidiary piers in side spans

In order to improve the vertical bending stiffness of cable-stayed bridges, several subsidiary piers are commonly used in side spans (Zhang, *et al.* 2003). To investigate the effect of the subsidiary piers in side spans on the flutter stability, different cases are analyzed, and the results are shown in Table 4 and Table 5.

Table 4 shows that the subsidiary piers help to improve the flutter stability of the bridge. It is due to the fact that as the subsidiary piers are used in side spans, the vertical bending and torsional frequencies are all increased, and also the vertical bending and torsional modes become more complicated. Therefore, the subsidiary piers in side spans are proved analytically to be both statically and aerodynamically favorable for the bridge. However, as seen in Table 5, due to little changes of modal frequencies, the critical wind speed is almost not affected by the location of the subsidiary pier in side spans.

5. Conclusions

In this paper, the method and solution procedure of nonlinear flutter stability analysis are firstly presented. Effects of some design parameters on the flutter stability of a cable-stayed-suspension hybrid bridge with main span of 1400 m are then investigated by nonlinear flutter stability analysis, some design parameters that significantly influence the flutter stability are pointed out, and the favorable structural system of the bridge is also discussed based on the wind stability. From the above investigation, some conclusions are drawn as follows

- (1) Increasing the cable sag is helpful for improving the flutter stability of cable-stayed-suspension hybrid bridges.
- (2) The short suspension portion is aerodynamically favorable for cable-stayed-suspension hybrid bridges.
- (3) The flutter stability of cable-stayed-suspension hybrid bridges can be greatly improved by

using outward inclined cable planes.

- (4) The composite deck is confirmed analytically to be favorable for improving the flutter stability of cable-stayed-suspension hybrid bridges, and therefore should be used in cable-stayed-suspension hybrid bridges.
- (5) The subsidiary piers in side spans are analytically proved to be aerodynamically favorable for cable-stayed-suspension hybrid bridges.

Acknowledgements

The writer would like to thank to Zhejiang Provincial Science Foundation of China under grant number 502118 for their financial support.

References

- Balsamo, F.P. and Drewery, R.M. (1989), "Inspection and rehabilitation of the John A. Roebling suspension bridge", *Proceedings of the 6th Annual International Bridge Conference*, Pittsburgh Pennsylvania.
- Boonyapinyo, V., Yamada, H. and Miyata, T. (1994), "Wind-induced nonlinear lateral-torsional buckling of cable-stayed bridges", *J. Struct. Eng.*, ASCE, **120**(2), 486-506.
- Bulson, D.S., Caldwell, J.B. and Seven, R.T. (1983), *Engineering Structures Development in the Twentieth Century*, The university of Bristol Press.
- Chen, A.R. and Song, J.Z. (2000), *Wind-resistant Research on the Runyang Bridge*, Research Report, Tongji University.
- Finzi, L. and Castllani, A. (1992), "Innovative structural system for 2 mile span suspension bridge", *Innovative Large Span Structures, IASS CSCE International Congress*, Toronto.
- Fumoto, K., Murakoshi, J., Hata, K. and Miyazaki, M. (2004), "A study on the aerodynamic characteristics of a new type of super long span bridge", *Proceedings of IABSE Congress*, Shanghai.
- Gimsing, N.J. (1992), "Design of a long-span cable-supported bridge across the Great Belt in Denmark", *Innovative Large Span Structures, IASS CSCE International Congress*, Toronto.
- Gimsing, N.J. (1997), *Cable-supported bridges-Concept & Design*, John Wiley & Sons Ltd., England.
- Hu, J. (2000), "Theoretical study of long-span cable-stayed-suspension bridges", Ph.D. thesis, Northern Jiaotong University, Beijing, China.
- Lin, T.Y. and Chow, P. (1991), "Gibraltar straits crossing- a challenge to bridge and structural engineers", *Struct. Eng., Int. J.*, IABSE, **1**(2).
- Meng, Y., Liu, D. and Sun, S.H. (1999), "Study on the design of long-span cable-stayed-suspension hybrid bridges", *J. Chongqing Jiaotong Institute*, **18**(4), 8-12.
- Namini, A.H. (1992), "Finite element-based flutter analysis of cable-suspended bridge", *J. Struct. Eng.*, ASCE, **118**(6), 1509-1526.
- Narasimha, D.L. (1991), "Bridges and flyovers", *Proceedings of the International Conference on Bridges and Flyovers*, Tata McGraw-Hill, New Delhi.
- Ostenfeld, K.H. (1992), "Innovative structural system for the Gibraltar Strait crossing project", *Innovative Large Span Structures, IASS CSCE International Congress*, Toronto.
- Sato H., Kusahara, S., Ogi, K., Kitagawa, M. and Ito, S. (2000), "Wind resistance of super long bridges in smooth flow", *Proceedings of the 16th Wind Engineering Symposium*, JAWWE, Nov.
- Scanlan, R.H. and Jones, N.P. (1990), "Aeroelastic analysis of cable-stayed bridges", *J. Struct. Eng.*, ASCE, **116**(2), 279-297.
- Xiao, R.C. (1998), "Design attempt of the linding east sea-route cable-stayed-suspension bridge", *Proceedings of the 13th National Conference on Bridge engineering*, Shanghai.
- Xiao, R.C. and Xiang, H.F. (1999), "Mechanics characteristics and economic performances study for cable-stayed-suspension bridges", *China Journal of Highway and Transportation*, **12**(3), 43-48.
- Xiao, R.C. (2000), "Research on the design of cable-stayed-suspension hybrid bridges", *China Civil Eng. J.*,

33(5), 46-51.

Zen, P., Zhong, T.Y. and Yan, G.P. (2002), "An study of dynamic characteristics for large-span cable-stayed-suspension bridges", *Chinese J. Comput. Mech.*, **19**(4), 472-475.

Zhang, X.J. and Sun, B.N. (2003), "Study of design parameters on flutter stability of cable-stayed bridges", *Wind and Struct.*, **6**(4), 279-290.

CC